

## Visualization and quantification of *Plasmodium falciparum* intraerythrocytic merozoites

Swati Garg<sup>1</sup> · Shalini Agarwal<sup>1</sup> · Surbhi Dabral<sup>1</sup> · Naveen Kumar<sup>2</sup> · Seema Sehwat<sup>2</sup> · Shailja Singh<sup>2</sup>

Received: 3 May 2014 / Accepted: 10 March 2015 / Published online: 5 April 2015  
© Springer Science+Business Media Dordrecht 2015

**Abstract** Malaria, a leading parasitic killer, is caused by *Plasmodium* spp. The pathology of the disease starts when *Plasmodium* merozoites infect erythrocytes to form rings, that matures through a large trophozoite form and develop into schizonts containing multiple merozoites. The number of intra-erythrocytic merozoites is a key-determining factor for multiplication rate of the parasite. Counting of intraerythrocytic merozoites by classical 2-D microscopy method is error prone due to insufficient representation of merozoite in one optical plane of a schizont. Here, we report an alternative 3-D microscopy based automated method for counting of intraerythrocytic merozoites in entire volume of schizont. This method offers a considerable amount of advantages in terms of both, ease and accuracy.

**Keywords** Plasmodium · Malaria · Merozoites · Schizonts · 2-D microscopy · 3-D microscopy · Imaris

*Plasmodium falciparum* a causative agent of human malaria is responsible for tremendous morbidity and mortality in many parts of the tropical world, especially Saharan and sub-Saharan regions (Richards and Beeson 2009). All the pathological symptoms of human malaria are directly associated with erythrocytic stage infection of *Plasmodium*. In this stage, parasite released from infected liver cells to the blood stream, invades erythrocytes and progress to form

rings and trophozoites. Mature trophozoites develop into schizonts that convert into segmentors by 3–6 rounds of nuclear and cytoplasmic division with 8–36 merozoites in each schizont. At the end of the cycle, the mature schizonts burst and release the merozoites to the blood stream again that in turn infect new erythrocytes and begin the new erythrocytic cycle again (Cowman and Crabb 2006; Singh and Chitnis 2012). The multiplicity rate of *Plasmodium* in erythrocytic cycle can be defined by the number of merozoites formed in an infected erythrocyte and their successful invasion to new erythrocytes. Severe malaria is associated with large parasite burdens (Chotivanich et al. 2000; Dondorp et al. 2005; Timms et al. 2001). The number of successfully invaded merozoites to erythrocyte determines the multiplication rate, which in turn determines the total parasite load (parasitemia). Multiplication rates can vary from 5 to 20 per cycle in various individuals depending upon the immune status of the patient (Gravenor et al. 1998; White and Krishna 1989). However, under in vitro culture conditions, where there is no immune pressure, the multiplication rate majorly depends on the number of merozoites formed within a schizont. Although the invasion rate can be scored by counting the number of ring-infected erythrocyte, no accurate and automated method is currently available for the direct estimation of intraerythrocytic merozoites (Chotivanich et al. 2000). The current study devises a novel, microscopy based method to enumerate number of merozoites per schizont which could be useful for evaluation of effects chemotherapeutics drugs have on proliferating erythrocytic stage parasites of *Plasmodium*.

Usually the invasion rate of the parasite and effect of chemotherapeutics is determined by scoring newly formed rings. However the effect seen could also be due to the change in number of merozoites formed in schizont in addition to their invasion ability (Mancio-Silva et al. 2013). During a

✉ Shailja Singh  
shailja.singh@snu.edu.in

<sup>1</sup> Malaria Group, International Centre for Genetic Engineering and Biotechnology (ICGEB), New Delhi 110067, India

<sup>2</sup> Department of Life Sciences, Shiv Nadar University, Gautam Budha Nagar 203207, UP, India

drug treatment, there is marked difference in number of intraerythrocytic merozoites that could be a consequence of change in the replication of parasites (Bargieri et al. 2013; Reilly et al. 2007). Therefore, the counting of number of merozoite nuclei per mature segmented schizont could provide the additional information on the effect seen in the form of reduced multiplication rate by the compounds. Many studies have already demonstrated the importance of the estimation of merozoites for explaining the reported observation. These studies have used the classical, microscopy counting of intraerythrocytic merozoites in giemsa stained smears of schizonts (Mancio-Silva et al. 2013). This method has limitations, such as, it is time consuming and data obtained comes from small sample count with manual error because of small size of merozoites. Due to unavailability of any automated technique to count number of merozoites we developed a novel, confocal based approach for counting the intraerythrocytic merozoites. We used volumetric imaging, also known as 3D imaging, by confocal microscopy to enumerate number of merozoites in the schizonts. Confocal images provided correct enumeration of merozoites in whole schizont volume and appropriate mathematic processing of these data allowed us to calculate the accurate number of merozoites in each schizonts.

## Results

### Counting of intraerythrocytic merozoites using 2-D and 3-D microscopy approaches

For estimation of intraerythrocytic merozoites by this method, the schizonts were smeared on a glass slide and stained for nucleic acid by DAPI and erythrocyte membrane by PKH26 dye and visualized under confocal microscope (Nikon A1 R). We acquired the images in XY plane (2D) as well as XYZ plane (volumetric acquisition, 3D) and counted number of merozoites within schizonts in both sets of images (Fig. 1). For both methods, the number of nuclei of mononucleated merozoites were counted for 100 schizonts. Counting was done from schizonts that have clearly segmented merozoites with limited overlap and with single pigmented residual body indicating single infection. To enumerate the number of number of nuclei formed during schigony, both 2D and 3D images were analyzed with IMARIS processing software. The animation capabilities provided by the latest version of Imaris software (version 6.2) offered us an automated quantization of intra-erythrocytic merozoites in both XY and XYZ-stacks images of schizonts. The 3D images were loaded into Imaris for a true 3D reconstruction and total number of merozoites were counted using Imaris Spots module in these 3D reconstructed images of schizonts (Fig. 1c).

### Comparison of the number of intraerythrocytic merozoites by 2-D and 3-D based microscopy counting

To compare the efficiency of the traditional 2D and the novel 3D approach for counting of intraerythrocytic merozoites, the number of merozoites were counted in 2D and 3D images of schizonts and plotted onto a bar graph. The average number of merozoites estimated in 3D reconstructed images was 22 per schizonts and no of merozoites estimated from 2D images was 15 per cell, although few schizonts had more than 30 merozoites (Fig. 2).

## Conclusion

Merozoites, within a schizont, are arranged in a 3D space. Counting of these merozoites in 2D could provide their number in one plane, while, at the same time, missing out at other merozoites lying in different plane. Therefore, it would be clever to develop a 3D approach to count merozoites lying in different planes and IMARIS, a newly developed imaging software, helped us to reconstruct 3D images and count number of intraerythrocytic merozoites with such an ease. In this study we have devised a novel, expeditious, 3D approach for counting intraerythrocytic merozoites that overcame the drawbacks associated with classical, manual counting.

We compared number of merozoites by 2D and 3D counting and found that average number of merozoites per schizont by 2D came out to be 15, while the same dataset, when analyzed by 3D, gave the average number of merozoites to be 22. The lower number of counts with 2D image of schizonts can be explained by the fact that, in XY plane counting, merozoites which are lying above or below the focal plane can be missed out. However in 3D image the merozoites are counted in total volume of schizonts so there was no chance of missing out of merozoites resulting in higher no of merozoites representing the correct numbers. Therefore this new method is able to produce more accurate data on number of intraerythrocytic merozoites and software makes the counting automated as well. This method can be useful for screening of compounds for testing their effect on multiplicity of *Plasmodium* parasites.

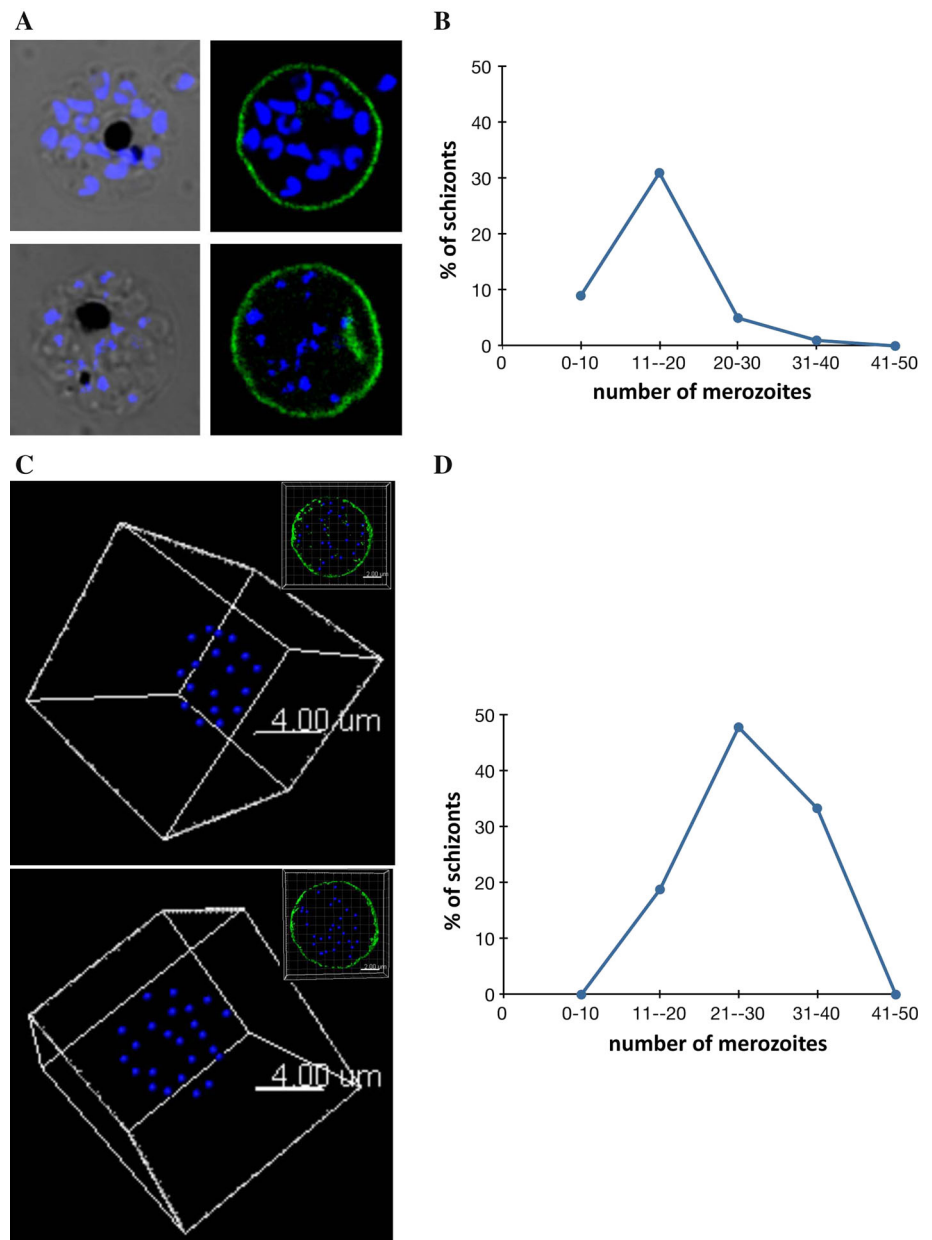
## Method

### In vitro culture of *P. falciparum*

Laboratory strain of *P. falciparum*, 3D7 was cultured in RPMI 1640 (Invitrogen, USA) supplemented with 27.2 mg/l of hypoxanthine (Sigma Aldrich, USA) and

**Fig. 1** Enumeration of merozoites within schizonts.

**a** Mature *P. falciparum* schizonts (46–48 hpi) were stained with membrane staining dye linker (Green) and nuclei staining dye, (DAPI, Blue). Since RBCs are enucleated, DAPI staining represents individual merozoites within schizonts and linker staining signifies RBC membrane of schizonts. **b** A graph was plotted for the number of merozoites in schizonts by classical, manual counting. **c** Merozoites were labelled with DAPI as and Phalloidin as described. A Z-stack series was captured using Nikon A1R confocal microscope. 3D animation was assembled using IMARIS software. Individual puncta representing a merozoite were detected within IMARIS software. The centre of each merozoite nuclei was represented by blue sphere. **d** A graph was plotted for the number of merozoites in schizonts by automated counting using IMARIS. (Color figure online)



0.5 % Albumax I (Invitrogen, USA) using O<sup>+</sup> RBCs in mixed gas environment (5 % O<sub>2</sub>, 5 % CO<sub>2</sub> and 90 % N<sub>2</sub>) as described previously and synchronized by sorbitol selection of rings.

**Quantification of intraerythrocytic merozoites**

Mature (46–48 hpi) schizonts were smeared on a glass slide, stained for nucleic acid by DAPI and erythrocyte

membrane by PKH-26 and visualized under confocal microscope. Images of the whole field were captured in 2-D as well as in 3D (>10 z-stacks). These datasets were then loaded into IMARIS software (Bitplane Inc.) Nuclei of schizonts were counted using “Spots” module. The RBCs, stained by PKH26, were counted using “Cell” module. All the counting data was then exported to excel. All the excel sheets were then compiled and further analyzed for the number of intraerythrocytic merozoite per schizont.

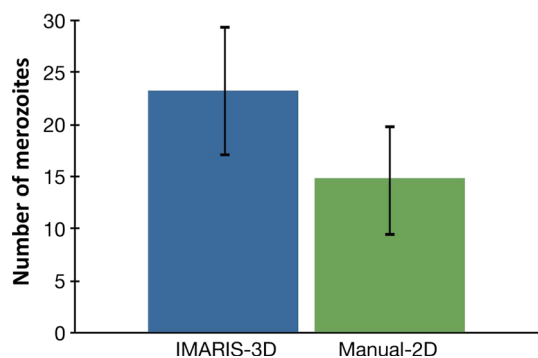


**Fig. 2** Comparison of intra-erythrocytic merozoite number evaluated by 2-D and 3-D methods. Intra-erythrocytic merozoites were counted using both classical 2-D and automated 3-D microscopy based method. The number of merozoites were plotted for the methods

**Acknowledgments** The authors thank Innovative Young Biotechnologist Award from DBT (to SS) for the upgradation of Confocal Microscope at ICGEB. Authors also thank ICGEB for access to Confocal Microscopy Facility and Imaris software.

**Conflict of interest** The authors declare no competing financial interests.

## References

Bargieri DY, Andenmatten N, Lagal V, Thiberge S, Whitelaw JA, Tardieux I, Meissner M, Ménard R (2013) Apical membrane

antigen 1 mediates apicomplexan parasite attachment but is dispensable for host cell invasion. *Nat Commun* 4:2552

Chotivanich K, Udomsangpetch R, Simpson JA, Newton P, Pukritayakamee S, Looareesuwan S, White NJ (2000) Parasite multiplication potential and the severity of falciparum malaria. *J Infect Dis* 181(3):1206–1209

Cowman AF, Crabb BS (2006) Invasion of red blood cells by malaria parasites. *Cell* 124(4):755–766

Dondorp AM, Desakorn V, Pongtavornpinyo W, Sahassananda D, Silamut K, Chotivanich K, Newton PN, Pitisuttithum P et al (2005) Estimation of the total parasite biomass in acute falciparum malaria from plasma PfHRP2. *PLoS Med* 2(10):390

Gravenor MB, van Hensbroek MB, Kwiatkowski D (1998) Estimating sequestered parasite population dynamics in cerebral malaria. *Proc Natl Acad Sci USA* 95(13):7620–7624

Mancio-Silva L, Lopez-Rubio JJ, Claes A, Scherf A (2013) Sir2a regulates rDNA transcription and multiplication rate in the human malaria parasite *Plasmodium falciparum*. *Nat Commun* 4:1530

Reilly HB, Wang H, Steuter JA, Marx AM, Ferdig MT (2007) Quantitative dissection of clone-specific growth rates in cultured malaria parasites. *Int J Parasitol* 37(14):1599–1607

Richards JS, Beeson JG (2009) The future for blood-stage vaccines against malaria. *Immunol Cell Biol* 87(5):377–390

Singh S, Chitnis CE (2012) Signalling mechanisms involved in apical organelle discharge during host cell invasion by apicomplexan parasites. *Microbes Infect* 14(10):820–824

Timms R, Colegrave N, Chan BH, Read AF (2001) The effect of parasite dose on disease severity in the rodent malaria *Plasmodium chabaudi*. *Parasitology* 123(Pt 1):1–11

White NJ, Krishna S (1989) Treatment of malaria: some considerations and limitations of the current methods of assessment. *Trans R Soc Trop Med Hyg* 83(6):767–777